# Accuracy Analysis and Improvement for Cooperative Industrial Robots

M. Wagner[1], A. Buschhaus[2], S. Reitelshöfer[2], P. Heß[3] and J. Franke[2]
[1]*Nuremberg Campus of Technology (NCT), Nuremberg Institute of Technology, 90429 Nuremberg, Germany*
[2]*Institute for Factory Automation and Production Systems (FAPS), Friedrich-Alexander-Universität Erlangen-Nürnberg (FAU), 91058 Erlangen, Germany*
[3]*Faculty of Mechanical Engineering and Building Services Engineering, Nuremberg Institute of Technology, 90489 Nuremberg, Germany*

Keywords: Accuracy, Calibration, Industrial Robots, Multi-robot Systems.

Abstract: The cooperative working of multiple robots on a common task often requires a high geometric accuracy. If such a system is modeled, many sources of error are present, which can quickly lead to inadequate process results. In order to avoid this, it is important to carry out a calibration in which deviations are determined. Subsequently, the model can be adapted to the actual conditions. In the scope of this work a kinematic calibration method for multi-robot systems is developed and realized with a robot setup consisting of two industrial robot arms. The accuracy of the robot system is significantly improved by the developed approach, which has been proven by experimental investigations.

## 1 INTRODUCTION

The accuracy of industrial robots has been under investigation for many years. Due to the current development of new industrial robot applications the accuracy gets more and more important. For example, high precision processes, like robot-based medical interventions (Boctor et al., 2004; Baron et al., 2010), are implemented using industrial robots. In addition, the number of processes programmed by offline programming rises and it is important to ensure a sufficient accuracy for these applications by matching the virtual model of the robot with the corresponding real robot. Therefore, many approaches for the improvement of the robot accuracy are developed. Since the changing of the mechanical structure is connected with a large expenditure, most commonly a calibration is done. Thus, the robot positioning accuracy is improved by detecting and compensating the error between the robot model and the real robot.

Another trend in industrial robotics is the use of multi-robot systems. Hence, applications can be improved or developed by a cooperation between multiple robots. The coordination between the involved robots may have four different levels (Wagner et al., 2014). In the first level, *no coordination* is done between the robots. Thus, the coordination must be considered in advance by the programmer. If the robots move independently, but receive individual signals from each other, this is called *asynchronous coordination*. As a result, for example, the transfer of workpieces can be coordinated. If the motions of the robots are linked by simple statements, this is called *semi-synchronous coordination*. The common lifting of heavy loads, as presented in (Müller et al., 2011) and in (Knepper et al., 2013), is an example for this kind of coordination. A more complex coordination of the movements is called *synchronous coordination*. In this case, for example, a common base movement is carried out while a robot is performing a superimposed processing movement, as shown in (Smits et al., 2008). Another example presented in (Wagner et al., 2014) is the cooperative processing by dividing the process movement in a tool and a workpiece movement.

More complex cooperative processes are often programmed offline, since the effort would otherwise be disproportionate. Also for cooperative processes a maximum match between the model and the real robot is very important in order to ensure a sufficient relative accuracy between the robots. An example for a cooperative process with a requirement of a high accuracy is the incremental sheet metal forming by two cooperating industrial robot arms (Meier et al., 2009). Also for the cooperative processing, presented in (Wagner et al., 2014), a high accuracy is necessary. Thus, a new approach for the improvement of the accuracy of multi-robot systems is



Wagner, M., Buschhaus, A., Reitelshöfer, S., Heß, P. and Franke, J.
Accuracy Analysis and Improvement for Cooperative Industrial Robots.
DOI: 10.5220/0006396805390546
In *Proceedings of the 14th International Conference on Informatics in Control, Automation and Robotics (ICINCO 2017) - Volume 2*, pages 539-546
ISBN: Not Available

presented in the scope of this paper.

This paper is structured as follows: Section 2 gives an overview about the current state of the art in kinematic calibration. Subsequently, the researched method for the accuracy improvement for cooperative industrial robots is presented in Section 3. The implementation of the approach with a setup consisting of two industrial robot arms is explained in Section 4. The last section concludes the paper.

# 2 KINEMATIC CALIBRATION

The aim of the kinematic calibration is the minimization of the deviation between the current path and the target path of the robot movement. The kinematic calibration can be carried out according to two basic principles (Day, 1996). On the one hand it can be done by an inline calibration using closed-loop correction (Buschhaus et al., 2016). Here, the error is detected and compensated during the processing. On the other hand the calibration can be performed by an open-loop correction (see Figure 1). In doing so, the error in the system is recorded once in a measuring process and the kinematic model is adapted accordingly.

According to (Elatta et al., 2004), the kinematic calibration consists of four sequential steps. First, the robot kinematics is modeled. Second, the necessary measurements are performed. Third, the calibration parameters are estimated based on the measured data. Finally, the calculated calibration parameters are used to adjust the kinematic model and thus to compensate the error. These four steps are explained in the following subsections.

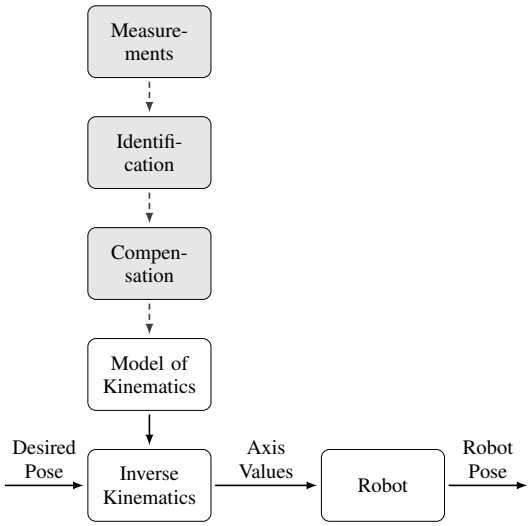


Figure 1: Open-loop correction method for industrial robots.

## 2.1 Modeling

The considered robot has a base coordinate system $\{B\}$ (see Figure 2) which is usually located inside of the robot base. Thus, the exact position of the base coordinate system is unknown. The pose of the flange $\{F\}$ results from the kinematics of the robot and is described by the transformation ${}^{B}\mathbf{T}_{F}$. For common applications the *tool center point* (TCP) $\{T\}$ is located in front of the flange. The equivalent transformation is denoted by ${}^{F}\mathbf{T}_{T}$.

Furthermore, two calibrations have to be performed in advance in order to achieve a sufficient accuracy. First, the exact base coordinate system $\{B\}$ must be determined. Thus, the base transformation ${}^{S}\mathbf{T}_{B}$ has to be measured indirectly and calculated based on geometric relations. Second, the transformation between the robot flange and the TCP ${}^{F}\mathbf{T}_{T}$ needs to be determined. Even if the tool is produced with high accuracy, there is still a relevant inaccuracy in its installation to the robot flange. If the base of the tool is not reachable by a mechanical measuring instrument, it has to be determined by a calibration procedure as well.

## 2.2 Measurements

During the measurements, the position of the TCP in the workspace of the robot is recorded. Various measurement methods, e.g. acoustic or visual sensors as well as coordinate measuring machines, can be used for this purpose. Most of the approaches use automatic theodolites, also known as laser tracker, due to their high precision (Alicia and Shirinzadeh, 2005; Nguyena et al., 2015).

The definition of the measurement positions depends on the respective applications. Thus, in (Alicia and Shirinzadeh, 2005) 80 positions are used to cover the range of motions for example. In order to reduce the number of positions, the optimal measuring posi-

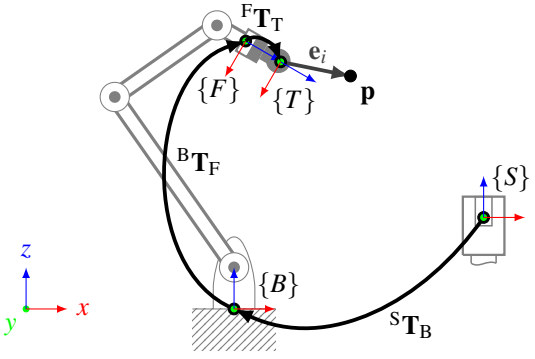


Figure 2: Coordinate systems at the accuracy analysis for industrial robots.

tions can be selected by using a genetic algorithm in (Aoyagi et al., 2010).

## 2.3 Identification

Each of the $N$ measured positions $\mathbf{p}_\mathrm{a} = (x_\mathrm{a}\ \ y_\mathrm{a}\ \ z_\mathrm{a})^\mathrm{T}$ can be compared with the corresponding desired position $\mathbf{p}_\mathrm{d} = (x_\mathrm{d}\ \ y_\mathrm{d}\ \ z_\mathrm{d})^\mathrm{T}$. Thus, an error vector $\mathbf{e} = (x_\mathrm{e}\ \ y_\mathrm{e}\ \ z_\mathrm{e})^\mathrm{T}$ can be calculated according to:

$$\mathbf{e}_i = \mathbf{p}_{\mathrm{a}_i} - \mathbf{p}_{\mathrm{d}_i}\ ,\quad i \in \{1,\ 2,\ \ldots,\ N\} \tag{1}$$

Furthermore, the error $\varepsilon$ of a position can be indicated by the distance between the two points by:

$$\varepsilon_i = ||\mathbf{e}_i|| = \\ = \sqrt{(x_{\mathrm{a}_i} - x_{\mathrm{d}_i})^2 + (y_{\mathrm{a}_i} - y_{\mathrm{d}_i})^2 + (z_{\mathrm{a}_i} - z_{\mathrm{d}_i})^2}\ , \tag{2}$$
$$i \in \{1,\ 2,\ \ldots,\ N\}$$

## 2.4 Compensation

In the final step of the kinematic calibration, the kinematic model of the robot is adapted according to the identified errors. The error consists of geometrical and non-geometrical errors (Elatta et al., 2004; Nguyena et al., 2015). Geometrical errors result from deviations in the link length or twist errors and can be determined relatively easy. Thus, e.g. the joint angle error can be estimated by a calibration, as shown in (Chen et al., 2008) by tracking a laser line in the robot workspace. Most of the approaches calculate the geometrical error based on the measurement of multiple robot positions with an external high precision measurement unit and a calculation of the deviation based on alorithms like extended Kalman filtering (Nguyena et al., 2015), root mean square (Alicia and Shirinzadeh, 2005) or non-linear least squares optimization (Lightcap et al., 2008; Aoyagi et al., 2010). Non-geometrical errors, such as gear backlash or join and link flexibility, are more difficult to determine. Some approaches use an artificial neural network to compensate this errors (Nguyena et al., 2015; Aoyagi et al., 2010). Other approaches try to model the non-geometrical errors, e.g. with a class of polynominals (Alicia and Shirinzadeh, 2005) or a Monte Carlo simulation (Lightcap et al., 2008).

# 3 APPROACH

For the cooperative processing, the relative accuracy between the robots is of importance. Thus, it is analyzed by measuring the absolute accuracy for both robots and by calculating the deviation between both measurements. Subsequently, the systematic error is compensated by an adaption of the kinematic model. According to the previous section, this section is divided into the same four subsections.

## 3.1 Modeling

At least two robots are required for cooperative processing (see Figure 3). In the following, the terms *workpiece guiding robot* and *tool guiding robot* are used for the involved robots. However, several robots can also guide the workpiece or the tool. Each robot has a transformation from its base to its flange, denoted by ${}^{\mathrm{B_T}}\mathbf{T}_{\mathrm{F_T}}$ and ${}^{\mathrm{B_W}}\mathbf{T}_{\mathrm{F_W}}$. Furthermore, each robot has a transformation from its flange to its TCP. This also applies to the reflector $\{R\}$ used for examining the accuracy by a laser tracker. The transformations to the center of the reflectors are ${}^{\mathrm{F_T}}\mathbf{T}_{\mathrm{R_T}}$ and ${}^{\mathrm{F_W}}\mathbf{T}_{\mathrm{R_W}}$. The transformation between the two robot base frames is denoted by ${}^{\mathrm{B_T}}\mathbf{T}_{\mathrm{B_W}}$. In addition, the transformations between the sensor base frame $\{S\}$ and the two robot base frames, denoted by ${}^{\mathrm{S}}\mathbf{T}_{\mathrm{B_T}}$ and ${}^{\mathrm{S}}\mathbf{T}_{\mathrm{B_W}}$, are relevant.

According to Section 2.1, a base and a tool calibration must also be carried out in advance for the cooperative approach. Thus, for each robot a base transformation, denoted by ${}^{\mathrm{S}}\mathbf{T}_{\mathrm{B_T}}$ and ${}^{\mathrm{S}}\mathbf{T}_{\mathrm{B_W}}$, as well as a reflector transformation, denoted by ${}^{\mathrm{F_T}}\mathbf{T}_{\mathrm{R_T}}$ and ${}^{\mathrm{F_W}}\mathbf{T}_{\mathrm{R_W}}$, are determined.

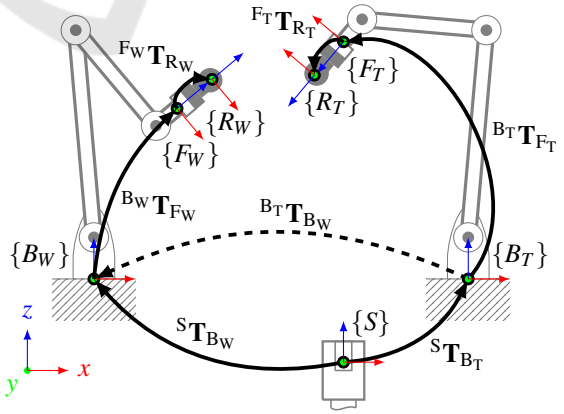


Figure 3: Coordinate systems at the accuracy analysis for cooperative processing.

### 3.2 Measurements

The investigation focuses on the part of the workspace which is relevant for the cooperative processing—the common workspace. In order to limit the amount of measurements, measuring points are equally distributed within the common workspace by an algorithm (see Figure 4). The algorithm runs with a constant step size from the bottom to the top of a box containing the workspace. In order to keep the robot paths to a minimum, the x-direction is toggled. Each iterated position is checked for reachability by inverse kinematics and the position will be added to the measurement positions, if it is reachable.

The algorithm generates programs for both robots that enables them to move the reflector to the absolute set poses of the accuracy analysis path. Due to the inaccuracies in the system, each robot movement has a deviation compared to the pre-defined path.

### 3.3 Identification

Based on the measurement results, the relative deviations between the measured positions and the desired positions is calculated via Equation 1 and Equation 2. However, the relative position between the two robots is essential for the cooperative process. Thus, the equations are adapted to the relative deviation between the two robot poses. The error vector $\mathbf{e}$ results from the difference between the measured tool position $\mathbf{p}_\mathrm{T}$ and the measured workpiece position $\mathbf{p}_\mathrm{W}$ by:

$$\mathbf{e}_i = \mathbf{p}_{\mathrm{T}_i} - \mathbf{p}_{\mathrm{W}_i}\,, \quad i \in \{1,\ 2,\ \ldots,\ N\} \tag{3}$$

The absolute error $\varepsilon$ at the position results from the distance between the two measured positions by:

$$\varepsilon_i = ||\mathbf{e}_i|| = \\ = \sqrt{(x_{\mathrm{T}_i} - x_{\mathrm{W}_i})^2 + (y_{\mathrm{T}_i} - y_{\mathrm{W}_i})^2 + (z_{\mathrm{T}_i} - z_{\mathrm{W}_i})^2}\,, \quad i \in \{1,\ 2,\ \ldots,\ N\} \tag{4}$$

Furthermore, a compensation transformation $\mathbf{T}_\mathrm{C}$ can be calculated from all of the deviations by the *Iterative Closest Point* (ICP) algorithm (Zhang, 1992). In the course of this, the transformation is determined by an interative minimization of the distances between the point clouds.

```
1:  procedure GENERATE PATHS(S_k)
2:      for z ← z_min, z_max do
3:          for y ← y_min, y_max do
4:              if toggle then
5:                  for x ← x_min, x_max do
6:                      if REACHABLE(x, y, z) then
7:                          commands → programs
8:                      end if
9:                  end for
10:             else
11:                 for x ← x_max, x_min do
12:                     if REACHABLE(x, y, z) then
13:                         commands → programs
14:                     end if
15:                 end for
16:             end if
17:             toggle ←!toggle
18:         end for
19:     end for
20: end procedure
```

Figure 4: Procedure for creating the robot paths with equally distributed measurement points for the accuracy analysis for cooperative processing.

### 3.4 Compensation

The open-loop correction method presented in Section 2 is modified in order to adapt the desired pose of the workpiece guiding robot (see Figure 5). For this purpose, the base transformation ${}^{\mathrm{B_T}}\mathbf{T}_{\mathrm{B_W}}$ is adapted using the compensation transformation $\mathbf{T}_\mathrm{C}$. The compensation transformation consists of a translation $\mathbf{t}_\mathrm{C} = (x_\mathrm{C}\ \ y_\mathrm{C}\ \ z_\mathrm{C})^\mathrm{T}$ and a rotation $\mathbf{r}_\mathrm{C} = (\alpha_\mathrm{C}\ \ \beta_\mathrm{C}\ \ \gamma_\mathrm{C})^\mathrm{T}$. Based on these parameters, the base transformation between the two robots can be modified by:

$${}^{\mathrm{B_T}}\mathbf{T}'_{\mathrm{B_W}} = {}^{\mathrm{B_T}}\mathbf{T}_{\mathrm{B_W}} \cdot \mathbf{T}_\mathrm{C} \tag{5}$$

Accordingly, a target pose for the workpiece guiding robot ${}^{\mathrm{B_W}}\mathbf{T}_\mathrm{P}$ can be determined by the target pose of the tool guiding robot ${}^{\mathrm{B_T}}\mathbf{T}_\mathrm{P}$ according to the equation:

$${}^{\mathrm{B_W}}\mathbf{T}_\mathrm{P} = (\mathbf{T}_\mathrm{C})^{-1} \cdot \left({}^{\mathrm{B_T}}\mathbf{T}_{\mathrm{B_W}}\right)^{-1} \cdot {}^{\mathrm{B_T}}\mathbf{T}_\mathrm{P} = \\ = \left({}^{\mathrm{B_T}}\mathbf{T}'_{\mathrm{B_W}}\right)^{-1} \cdot {}^{\mathrm{B_T}}\mathbf{T}_\mathrm{P} \tag{6}$$

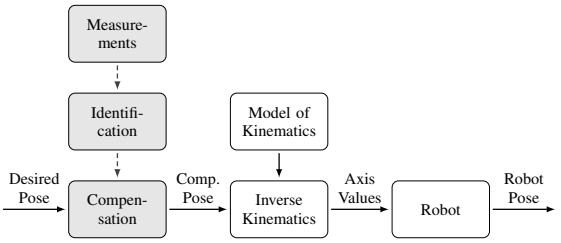


Figure 5: Open-loop correction method for the desired pose of cooperative industrial robots.

# 4 IMPLEMENTATION & RESULTS

The previously described approach is implemented with a robot setup consisting of two industrial robot arms. The setup is presented in the next subsection. Subsequently, the realization of the preliminary calibrations is explained. In the last subsection the realization of the measurements and the resulting data is presented.

## 4.1 Setup

The robotic system used for the investigation consists of two *KUKA KR 6 R900 sixx* industrial robot arms (see Figure 6). They are mounted next to each other with a distance of approximately 1325 mm in y-direction. Each robot arm consists of six axis and a position repeatability of $\pm 0.03$ mm according to manufacturer specifications.

The laser tracker *API R-20 Radian* is used as an external measuring device. It is placed in front of the robots to be able to measure within the entire common workspace. Each robot has a reflector mounted to its flange via an adapter plate.

## 4.2 Calibrations

According to Section 3.1, two calibrations have to be performed before the measurements. First, the base coordinate systems of the robots have to be determined. They are measured by mounting a reflector on the rotating part of the robot next to the first and the second rotational axis. For both axes a measurement is performed by rotating the axes. This results in a circular path whose center point lies in the rotational axis. The actual robot base can be determined via the intersection of the resulting rotational axes.

Furthermore, the transformation between the two robots base coordinate systems can be determined by:

$$ {}^{B_T}\mathbf{T}_{B_W} = \left({}^{S}\mathbf{T}_{B_T}\right)^{-1} \cdot {}^{S}\mathbf{T}_{B_W} \tag{7} $$

The resulting base transformation for the examined setup consists of a translation of $\mathbf{t}_B = (3.18 \quad -1319.28 \quad 0.17)^T$ in mm and a rotation of $\mathbf{r}_B = (0.00 \quad 0.01 \quad 0.26)^T$ in degree.

Second, the translation between the flange and the mounted reflector needs to be determined. Since the fixing adapter is produced with a very high accuracy in radial direction, a low eccentricity is assumed. Therefore, only the offset in z-direction is estimated by the calibration. For this purpose, the robot performs a pitch rotation around its flange axis. Thereby, a circular path of the reflector can be recorded. The z-offset is equivalent to the radius of the fitting circle. The resulting values for the considered setup are $z_{R_T} = 36.79$ mm for the tool guiding robot and $z_{R_W} = 36.71$ mm for the workpiece guiding robot.

## 4.3 Measurements & Data

The measurement paths for both robots are generated according to Section 3.2. The resulting programs contain movements inside the common workspace of both robots, which are aligned on a uniformly distributed grid (see Figure 7). After each movement command the program contains a wait-command to ensure a measurement at the desired position. The generated path consist of a total of 472 measurement positions.

Based on the measurement results, the relative deviations between the matching positions can be calculated by Equation 3 and Equation 4. Figure 8(a)-8(c) show the resulting deviations divided in x-, y- and z-direction. The magnitude of the deviation is directly proportional to the length of the line and the lines are colored according to a heatmap, which is shown in Figure 8(d).

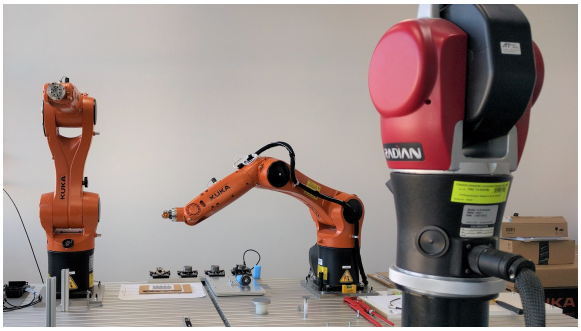

Figure 6: Setup for the accuracy analysis for cooperative industrial robots.

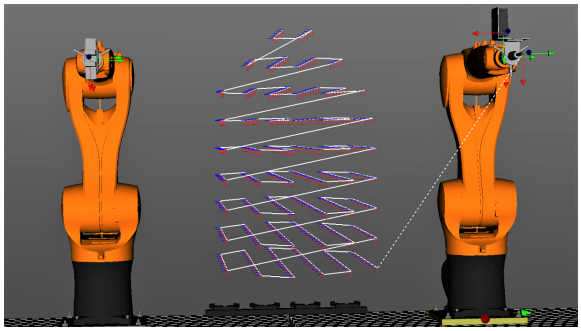

Figure 7: Generated robot path for the tool guiding robot for the accuracy analysis.

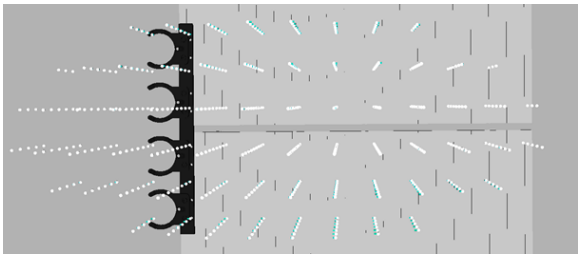

(a) Deviation in x-direction.

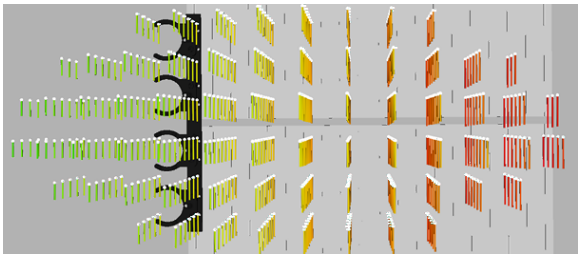

(b) Deviation in y-direction.

(c) Deviation in z-direction.

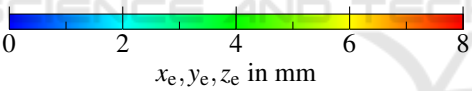


(d) Heatmap.

Figure 8: Accuracy maps with scaled deviations colored by a heat map depending on the absolute value.

Furthermore, the deviation values are summarized in diagrams (see Figure 9) in order to get a better overview. Here, all measurement points are listed in sequence. Each axial direction $(x_e, y_e, z_e)$ is presented in a separate diagram as well as the absolute error $\varepsilon$.

The distribution of the deviations before the compensation is presented in Table 1.

The deviation in x- and z-direction varies in the range between about -1.0 mm and 1.0 mm. A comparatively large negative deviation in the y-direction is obvious, which presumably is due to the oppositeness of the two robots in this direction. This deviation is decisive for the absolute error with a maximum of more than 8.0 mm. The standard deviations before the compensation are in the range of 0.40 mm to 0.96 mm.

Table 1: Distribution of relative positional deviations for the cooperative robot system.

| | $\bar{\mathbf{e}}$ (mm) | $\min(\mathbf{e})$ (mm) | $\max(\mathbf{e})$ (mm) | $\sigma(\mathbf{e})$ (mm) |
|---|---|---|---|---|
| $x_e$ | -0.0262 | -1.0007 | 0.9037 | 0.4044 |
| $y_e$ | -5.8465 | -8.1463 | -3.6525 | 0.9559 |
| $z_e$ | 0.0087 | -1.2508 | 1.1629 | 0.6119 |
| $\varepsilon$ | 5.8925 | 3.6713 | 8.1544 | 0.9547 |

According to Section 3.4, a compensation is performed. The resulting compensation transformation for the considered setup consists of a translation of $\mathbf{t}_C = (-1.81 \quad 6.96 \quad 1.41)^T$ in mm and a rotation of $\mathbf{r}_C = (0.16 \quad 0.00 \quad 0.12)^T$ in degree. The deviations after the compensation are also shown in the diagrams (see Figure 9). Table 2 shows the distribution of the deviations after the compensation. The mean error vector tends to zero and all deviations are less than 0.8 mm. The standard deviations after the compensation are between 0.14 mm and 0.31 mm. In order to provide better comparability, the data is displayed in a box-and-whisker diagram (see Figure 10).

## 5 CONCLUSIONS

In the scope of this paper an approach for the improvement of the accuracy for cooperative industrial robots is developed. Thus, the robots are examined by means of a high-precision external measuring device. On the one hand, the approach includes the creation of robot programs for the measurement. On the other hand, the estimation of an error compensation is presented. The approach is implemented with a robot system with two industrial robot arms for validation. The comparison of the deviations before and after the compensation shows a significant reduction of about 90 %. In addition, the variation is significantly reduced in comparison to the deviations without compensation.

Table 2: Distribution of relative positional deviations for the cooperative robot system after the compensation.

| | $\bar{\mathbf{e}}'$ (mm) | $\min(\mathbf{e}')$ (mm) | $\max(\mathbf{e}')$ (mm) | $\sigma(\mathbf{e}')$ (mm) |
|---|---|---|---|---|
| $x'_e$ | -0.0001 | -0.3687 | 0.6136 | 0.1889 |
| $y'_e$ | 0.0001 | -0.5031 | 0.4041 | 0.2088 |
| $z'_e$ | 0.0000 | -0.7086 | 0.6213 | 0.3077 |
| $\varepsilon'$ | 0.3905 | 0.0223 | 0.7938 | 0.1456 |

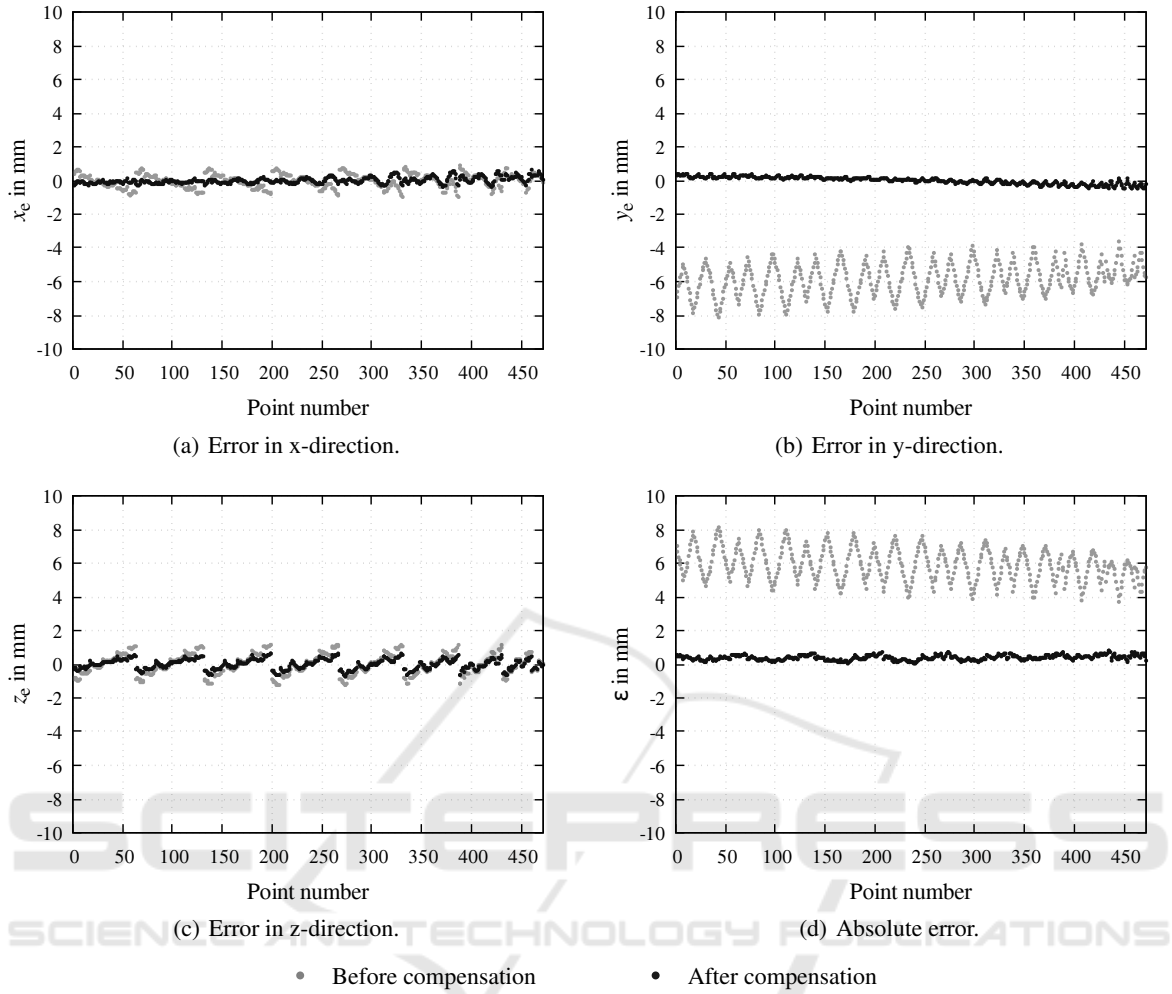


Figure 9: Deviations at the different measurement positions.

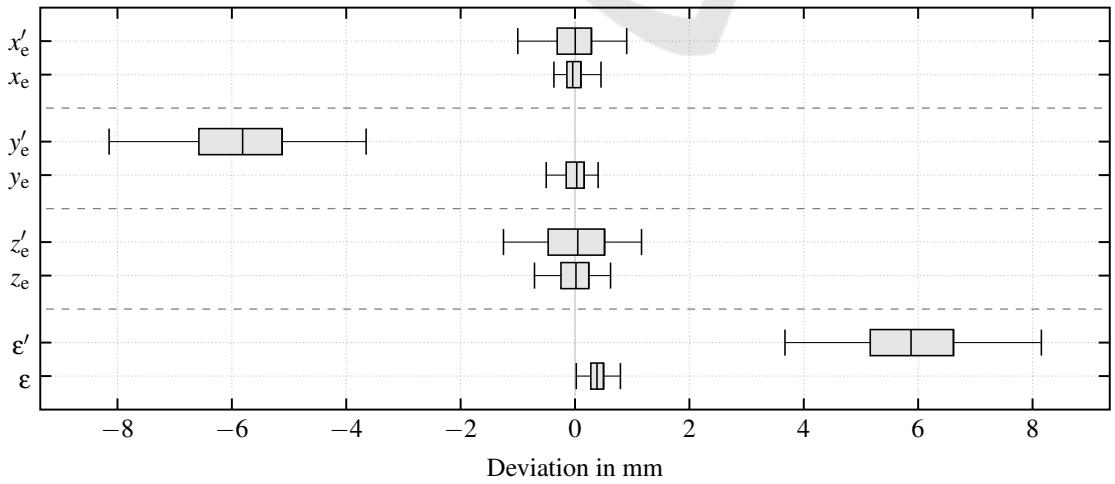


Figure 10: Box-and-whisker diagram of relative positional deviations for the cooperative robot system.

## REFERENCES


Alicia, G. and Shirinzadeh, B. (2005). A systematic technique to estimate positioning errors for robot accuracy improvement using laser interferometry based sensing. In *Mechanism and Machine Theory*, volume 40, pages 879–906. Elsevier.

Aoyagi, S., Kohama, A., Nakata, Y., Hayano, Y., and Suzuki, M. (2010). Improvement of robot accuracy by calibrating kinematic model using a laser tracking system-compensation of non-geometric errors using neural networks and selection of optimal measuring points using genetic algorithm. In *Proceedings of the IEEE/RSJ International Conference on Intelligent Robots and Systems (IROS 2010)*, pages 5660–5665. IEEE.

Baron, S., Eilers, H., Munske, B., Toennies, J. L., Balachandran, R., Labadie, R. F., Ortmaier, T., and III, R. J. W. (2010). Percutaneous inner-ear access via an image-guided industrial robot system. In *Proceedings of the Institution of Mechanical Engineers, Part H: Journal of Engineering in Medicine*, volume 224, pages 633–649. SAGE.

Boctor, E. M., Fischer, G., Choti, M. A., Fichtinger, G., and Taylor, R. H. (2004). A dual-armed robotic system for intraoperative ultrasound guided hepatic ablative therapy: a prospective study. In *Proceedings of the IEEE International Conference on Robotics and Automation (ICRA 2004)*, volume 3, pages 2517–2522. IEEE.

Buschhaus, A., Grünsteudel, H., and Franke, J. (2016). Geometry-based 6d-pose visual servoing system enabling accuracy improvements of industrial robots. In *Proceedings of the International Conference on Advanced Mechatronic Systems (ICAMechS 2016)*, pages 195–200. IEEE.

Chen, H., Fuhlbrigge, T., Choi, S., Wang, J., and Li, X. (2008). Practical industrial robot zero offset calibration. In *Proceedings of the IEEE International Conference on Automation Science and Engineering (CASE 2008)*, pages 516–521. IEEE.

Day, C. P. (1996). Robot accuracy issues and methods of improvement. In *Progress in Robotics and Intelligent Systems*, volume 2, pages 90–108. Intellect Books.

Elatta, A., Gen, L., Zhi, F., Daoyuan, Y., and Fei, L. (2004). An overview of robot calibration. In *Information Technology Journal*, volume 3, pages 74–78. Asian Network for Scientific Information.

Knepper, R. A., Layton, T., Romanishin, J., and Rus, D. (2013). Ikeabot: An autonomous multi-robot coordinated furniture assembly system. In *Proceedings of the IEEE International Conference on Robotics and Automation (ICRA 2013)*, pages 855–862. IEEE.

Lightcap, C., Hamner, S., Schmitz, T., and Banks, S. (2008). Improved positioning accuracy of the pa10-6ce robot with geometric and flexibility calibration. In *IEEE Transactions on Robotics*, volume 24, pages 452–456. IEEE.

Meier, H., Buff, B., Laurischkat, R., and Smukala, V. (2009). Increasing the part accuracy in dieless robot-based incremental sheet metal forming. In *CIRP Annals - Manufacturing Technology*, pages 233–238. Elsevier.

Müller, R., Esser, M., and Janssen, M. (2011). Integrative path planning and motion control for handling large components. In *Proceedings of the 4th International Conference on Intelligent Robotics and Applications (ICIRA 2011)*, pages 93–101. Springer-Verlag, Berlin, Germany.

Nguyena, H.-N., Zhoua, J., and Kang, H.-J. (2015). A calibration method for enhancing robot accuracy through integration of an extended kalman filter algorithm and an artificial neural network. In *Neurocomputing*, volume 151, pages 996–1005. Elsevier.

Smits, R., Laet, T. D., Claes, K., Bruyninckx, H., and Schutter, J. (2008). itasc: a tool for multi-sensor integration in robot manipulation. In *Proceedings of the IEEE International Conference on Multisensor Fusion and Integration for Intelligent Systems*, pages 426–433. IEEE.

Wagner, M., Heß, P., and Reitelshöfer, S. (2014). Automated programming of cooperating industrial robots. In *Proceedings for the joint conference of 45st International Symposium on Robotics (ISR 2014) und 8th German Conference on Robotics (ROBOTIK 2014)*, pages 129–136. VDE-Verlag, Berlin, Germany.

Zhang, Z. (1992). Iterative point matching for registration of free-form curves. In *Technical Report RR-1658*. INRIA Sophia Antipolis, Valbonne Cedex, France.